

SENSITIVITY TESTS WITH A BIOSPHERE MODEL BASED ON BATS, SUITABLE FOR COUPLING WITH A SIMPLE CLIMATIC MODEL

S. H. Franchito, V. Brahmananda Rao & M. A. Varejão-Silva

A biosphere model based on the Biosphere Atmosphere Transfer Scheme (BATS) suitable for coupling with a simple climate model is described. In this model the equations of BATS are adapted to the energy flux formulations of the statistical-dynamical model developed by Franchito & Rao (Climatic Change, 22:1-34; 1992). In this work the land surface model was run to perform sensitivity tests regarding the behaviour of the model variables with respect to prescribed model parameters and contrasting vegetation types, such as evergreen broadleaf forest and short grass. The results show that the soil surface temperature increases with the decrease of the fractional area of vegetation cover due to the lower surface solar radiation flux absorption in both types of vegetation. As the water interception increases the wet foliage air layer prevents the evaporation of the soil water, so that there is an increase of the ground surface temperature. The surface temperature is lower in the forest than in the case of short grass due to the surface roughness effect. In the case of dry soil the available energy increases with the increase of the fractional area of vegetation cover because the latent heat flux increases quickly and the sensible heat flux decreases slowly. In the situation of fully wet soil the available energy dependence on the interception is reduced due to the effect of water evaporation at the ground surface that increases the latent heat flux, even if the interception is small or nil. A factor ζ is inserted in the expression that gives the fractional area of the leaf canopy cover by water in order to take into account the effect of the part of vegetation predominantly porous. The lower values of ζ give better results regarding the component terms of the evapotranspiration. However, the total flux of water vapor to atmosphere does not change with ζ . Sensitivity tests are made with respect to the factor Y introduced in the expression of the water vapor flux to the atmosphere in order to adjust the partitioning of the available energy into latent and sensible heat. The results show that the latent (sensible) heat increases (decreases) with the increase in Y . Although the variation of Y modifies the Bowen's ratio there is no change of the evapotranspiration partitioning into its components.

Key words: Biosphere model based on BATS; Statistical-dynamical model; Sensitivity tests with a biosphere model.

TESTES DE SENSIBILIDADE COM UM MODELO DE BIOSFERA BASEADO NO ESQUEMA BATS, ÚTIL PARA SER ACOPLADO A UM MODELO CLIMÁTICO SIMPLES - *Um modelo de biosfera baseado no esquema BATS (Biosphere Atmosphere Transfer Scheme) útil para ser acoplado a um modelo climático simples é descrito. Neste modelo as equações do esquema BATS são adaptadas às formulações dos fluxos de energia do modelo estatístico-dinâmico desenvolvido por Franchito & Rao (Climatic Change, 22: 1-34; 1992). Neste trabalho, o modelo de processos de superfície foi rodado para realizar testes de sensibilidade referentes ao comportamento das variáveis do modelo com respeito a parâmetros prescritos e tipos de vegetação contrastantes, tais como floresta perenifólia e gramíneas. Os resultados mostraram que a temperatura da superfície do solo aumenta com o decréscimo da fração da cobertura vegetal devido à menor absorção do fluxo de radiação solar na superfície em ambos os tipos de vegetação. A medida que a interceptação aumenta a camada de ar na folhagem úmida impede a evaporação de água no solo, de forma que há um aumento da temperatura da superfície do solo. A temperatura da superfície é menor sob a floresta perenifólia do que sob gramíneas baixas devido ao efeito da rugosidade da superfície. No caso de solo seco a energia disponível aumenta quanto maior for a fração de cobertura vegetal pois o fluxo de calor latente aumenta rapidamente enquanto que o fluxo de calor sensível reduz-se mais lentamente. Na situação de solo plenamente abastecido de água, a dependência da energia disponível em relação à interceptação diminui devido ao efeito da evaporação de água à superfície do solo, a qual aumenta o fluxo de calor latente mesmo que a interceptação é pequena ou nula. Um fator ζ foi inserido na expressão referente à fração da folhagem coberta pela água interceptada para levar em conta o efeito da parte da vegetação predominantemente porosa. Melhores resultados dos cálculos dos termos componentes da evapotranspiração foram obtidos com menores valores de ζ . Contudo, o fluxo total de vapor d'água para a atmosfera não se altera com ζ . Foram realizados testes de sensibilidade com respeito ao fator Y , introduzido na expressão do fluxo de vapor d'água para a atmosfera para ajustar a partição da energia disponível em calor sensível e latente. Os resultados mostraram que o fluxo de calor latente (sensível) aumenta (decrece) quanto maior for Y . Embora a variação de Y modifica a razão de Bowen, não há alteração na partição da evapotranspiração em seus termos componentes.*

Palavras-chave: Modelo de biosfera baseado no esquema BATS; Modelo estatístico-dinâmico; Testes de sensibilidade com um modelo de biosfera.

Instituto Nacional de Pesquisas Espaciais, INPE
CP 515, 12201-970, São José dos Campos, SP
E-mail: fran@met.inpe.br

INTRODUCTION

Recently, much attention in climate modeling has been directed towards the parameterizations of the interaction between the vegetation and the atmospheric processes. The different vegetation types and their distribution over the Earth's surface influence directly the surface-atmosphere interface processes such as the aerodynamical properties involving the canopy structure and the surface roughness. These affect the turbulence and the wind profile at the atmospheric layer near the surface whereas the energetic properties, such as the absorptivity and reflectivity, modify the energy fluxes at the surface. The biological properties, which influence the transpiration rate, the photosynthesis, and, consequently, the growth of the plants are also important. The vegetative cover has an important role in the climate system because it affects directly the exchanges of water, energy and momentum between the land-surface and the atmosphere. Thus, the substitution of a large area of some type of vegetation cover by another one with different properties may cause significant impacts in the exchanges between the land-surface and the atmosphere, and, consequently, in the climate. It has been suggested that man-induced processes, such as deforestation, desertification and urbanization may have significant effects on local, regional, and perhaps global climate (Sagan et al., 1979; Budyko, 1982).

General circulation models (GCMs) are useful tools in studies of climatic change due to land-surface alterations (Dickinson & Henderson-Sellers, 1988; Nobre et al., 1991; Henderson-Sellers et al., 1993; Dirmeyer & Shukla, 1994; and many others). During the last decade, numerical models of the biosphere, which include an adequate description of surface processes, have been developed and incorporated into GCMs in order to study the interaction between the vegetation and climate. The principal biosphere models for GCMs are: the Biosphere-Atmosphere Transfer Scheme (BATS) (Dickinson et al., 1986), the Simple Biosphere Model (SiB) (Sellers et al., 1986), the Bare Essentials Model (Pitman, 1988), and the Interaction between Soil, Biosphere, and Atmosphere (ISBA) (Noilhan & Planton, 1989).

Although the GCMs are the most powerful tools used in climatic change studies, an efficient way of obtaining preliminary ideas of the climatic effects is to use a simple climate model, such as a statistical-dynamical model (SDM). Simple climate models have been and will continue to be useful tools in climatic research because they are

computationally economical and their behaviour are easier to analyse. A parameterization of the feedback mechanisms which link the land-surface state to the atmospheric processes suitable for a simple model was proposed by Gutman et al. (1984). The method was based on making the land surface albedo and the water availability parameter dependent on the ratio between the annual radiation balance and the annual precipitation, called radiative index of dryness. They incorporated this parameterization in a hemispheric quasi-geostrophic SDM, which was applied only for the Northern Hemisphere. Franchito & Rao (1992) applied this method to obtain similar parameterizations for the Southern Hemisphere and included them in a global primitive equation SDM. A more sophisticated scheme of the biosphere, where the equations of BATS were adapted to the formulation of the energy fluxes proposed by Saltzman & Vernekar (1971), was developed by Zhang (1994). In that study, Zhang (1994) only made tests with the vegetation model. Recently, Varejão-Silva et al. (1998) coupled this biosphere model to the SDM developed by Franchito & Rao (1992) in order to study the climatic impact due the Amazonian deforestation and the African desertification.

The purpose of the present work is to use the vegetation model adapted to the formulation of the energy fluxes of the SDM developed by Franchito & Rao (1992) in order to perform sensitivity tests concerning the behaviour of model variables with respect to different prescribed model parameters and contrasting vegetation types, such as evergreen broadleaf forest and grassland. In a previous study the coupled model, where the vegetation is an interactive element of the climate system, is used to simulate the mean annual zonally averaged climate variables (Varejão-Silva et al., 1998).

THE BIOSPHERE MODEL

The biosphere model is similar to that proposed by Zhang (1994). In this model the equations of BATS are adapted to the energy fluxes formulations proposed by Saltzman & Vernekar (1971). The model is based on the parameterizations of the energy balances at the earth's surface, the foliage, and the foliage air layer, and the moisture balance of the foliage air layer (Fig. 1). As can be seen in Varejão-Silva et al. (1998), the parameterizations of diabatic heating in the SDM developed by Franchito &

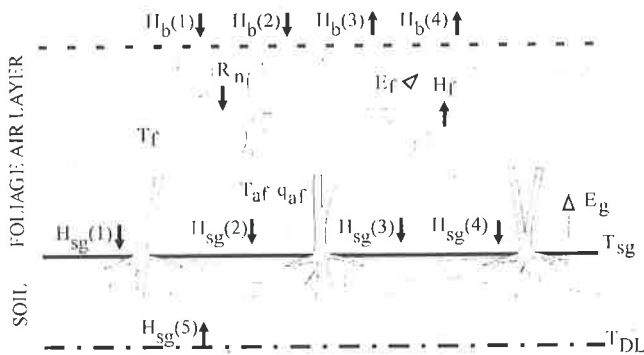


Figure 1 - The biosphere model. $H_{sv}(i)$, $i=1, \dots, 5$ are the energy fluxes at the soil surface: shortwave and net longwave radiation fluxes, the sensible and latent heat fluxes, and the subsurface conduction flux, respectively; and $H_b(i)$, $i=1, \dots, 4$ are the energy fluxes in the foliage air layer: shortwave and net longwave radiation fluxes, and the sensible and latent heat fluxes, respectively.

Figura 1 - O modelo da biosfera. $H_{sv}(i)$, $i=1, \dots, 5$ são os fluxos de energia na superfície do solo: fluxos de radiação de onda curta e onda longa, fluxos de calor sensível e latente, e condução para a sub-superfície, respectivamente; e $H_b(i)$, $i=1, \dots, 4$ são os fluxos de energia na camada de ar na folhagem: fluxos de radiação de onda curta e de onda longa, e fluxos de calor sensível e latente, respectivamente.

Rao (1992) are based on those proposed by Saltzman & Vernekar (1971). This allows the coupling of the models.

a) The energy balance at the earth's surface

The energy balance at the earth's surface assumes that the net heat fluxes towards the air-soil interface is zero:

$$H_{sv}(1) + H_{sv}(2) + H_{sv}(3) + H_{sv}(4) + H_{sv}(5) = 0 \quad (1)$$

where $H_{sv}(i)$, $i=1, \dots, 5$ correspond to the shortwave radiation and the net longwave radiation fluxes, the sensible and latent heat fluxes, and the subsurface conduction flux, respectively. The formulations of these fluxes are given in Tab. 1, where σ_f is the fractional area of the vegetation cover; χ e r_a are the opacity and the albedo of the atmosphere, respectively; r_s , the soil albedo; R_o , the solar radiation flux incident at the top of the atmosphere; σ_B , the Stephan-Boltzman constant; v_1 is the downward longwave radiation factor; T_2 , is the temperature at 500 hPa; T_{sv} , T_f , T_{af} and T_{DL} , are the surface, foliage, foliage air-layer, and subsurface temperatures, respectively; q_{gs} , the saturated mixing ratio of water vapor at surface; q_{af} , the water vapor mixing ratio of the foliage air layer; f_g , the water availability

at the earth's surface; L and c_p are the latent heat of vaporization and the specific heat capacity for dry air, respectively; and k_v is the factor proportional to the soil conductive capacity.

The fractional area of the vegetation cover (σ_f) is a variable which depends on the season. Its parameterization in BATS is made as a function of subsurface temperature (T_{DL}):

$$\begin{aligned} \sigma_f &= \sigma_{fmax} && \text{if } T_{DL} > 298 \text{ K} \\ \sigma_f &= \sigma_{fmax} - \Delta\sigma_f && \text{if } T_{DL} < 273 \text{ K} \\ \sigma_f &= \sigma_{fmax} - \Delta\sigma_f [1 - F_{sens}(T_{DL})] && \text{in the other cases} \end{aligned} \quad (2)$$

The maximum fractional vegetation cover (σ_{fmax}) and the seasonal range of vegetation cover ($\Delta\sigma_f$) are given in BATS and the seasonality factor $F_{sens}(T)$ has the same formulation as in BATS:

$$F_{sens}(T) = 1 - 0.0016(298 - T)^2 \quad (3)$$

In Tab. 1, the atmospheric emissivity (ϵ_a) is assumed constant ($\epsilon_a = 0.95$) and the emissivities of the foliage (ϵ_f) and soil (ϵ_s) are given, respectively, by (Zhang, 1994):

$$\epsilon_f = 1 - r_{nr} \quad (4)$$

$$\epsilon_s = 1 - 2 r_s \quad (5)$$

where r_{nr} is the longwave albedo of the foliage given in BATS, and

$$h = \rho_a c_p C_D [(1 - \sigma_f) V_a + \sigma_f U_{af}] \quad (6)$$

$H_{sv}(1) = (1 - \sigma_f)(1 - \chi)(1 - r_s)R_o$ $H_{sv}(2) = \sigma_B \{ (1 - \sigma_f)(v_1 T_2^4 - T_{sv}^4)/\psi_1 + \sigma_f(T_f - T_{sv})/\psi_2 \}$ $H_{sv}(3) = h (T_{af} - T_{sv})$ $H_{sv}(4) = h L f_g (q_{af} - q_{gs})/c_p$ $H_{sv}(5) = -k_v (T_{sv} - T_{DL})$
--

Table 1 - Functional forms of the energy fluxes at the soil surface.

Tabela 1 - Formas funcionais dos fluxos de energia na superfície do solo.

The drag coefficient C_D is given by:

$$C_D = \sigma_f C_{DV} + (1 - \sigma_f) C_{DL} \quad (7)$$

where $C_{DL} = [k_{vk} / \ln(z_l/z_{oL})]^2$ and $C_{DV} = [k_{vk} / \ln(z_l/z_{oV})]^2$ are the drag coefficient over land and over vegetation, respectively. In the equations above, ρ_a is the dry air density; $k_{vk} = 0.4$ is the Von Kármán constant; $z_{oL} = 0.01$ m is the roughness length of land; z_{oV} , the roughness length of vegetation (given in BATS); and $z_l = 10$ m is the height of the anemometer level. Following the same parameterization given in BATS: $U_{af} = V_a (C_D)^{1/2}$, where V_a and U_{af} are the wind speed at the anemometer level and the wind speed in the foliage air layer, respectively.

b) The energy balance of the foliage air layer

Following the same parameterization proposed by Zhang (1994), the energy balance of the foliage air layer assumes that the heat fluxes from the ground [$H_{sv}(3)$] and from the foliage (H_f) must be balanced by the heat flux to the atmosphere [$H_b(3)$]:

$$H_b(3) = H_f + H_{sv}(3) \quad (8)$$

where $H_b(3)$ is given in Tab. 2 and H_f has the same formulation of BATS:

$$H_f = \sigma_f L_{sai} \rho_a c_p (T_f - T_{af}) / r_{la} \quad (9)$$

The factor $[b_2(T_{af} - T_2) + c_2]$ that appears in $H_b(3)$ is the same as the parameterization of this flux proposed by Saltzman & Vernekar (1971), with $b_2 = 4.03 \text{ J m}^{-2} \text{ s}^{-1} \text{ K}^{-1}$ and $c_2 = -95 \text{ J m}^{-2} \text{ s}^{-1}$. In the present paper, $c_2 = -115 \text{ J m}^{-2} \text{ s}^{-1}$,

$$H_b(1) = \sigma_f (1 - \chi)(1 - r_a) R_o$$

$$H_b(2) = \sigma_f \sigma_B [(T_{sv}^4 - T_f^4)/\psi_2 + (v_l T_2^4 - T_f^4)/\psi_6]$$

$$H_b(3) = (C_D/C_{D0}) [b_2(T_{af} - T_2) + c_2]$$

$$H_b(4) = (q_{af}/q_{ns}) [e_2 H_b(3) + f_2]$$

Table 2 - Functional forms of the energy fluxes in the foliage air layer.

Tabela 2 - Formas funcionais dos fluxos de energia na camada de ar na folhagem.

which is more proper for the coupling with the SDM developed by Franchito & Rao (1992) (Varejão-Silva et al., 1998). Also, regarding the formulation of $H_b(3)$, $C_{D0} = 0.003$ is a reference value of the drag coefficient, which is used in correction factor (C_D/C_{D0}) proposed by Zhang (1994), in order to include the effect of the vegetation. The resistance to heat or moisture transfer through the laminar boundary layer at the foliage surface (r_{la}), which appears in Eq. (9), has the same formulation as in BATS:

$$r_{la} = C_f (U_{af})^{1/2} (1/D_f)^{1/2} \quad (10)$$

where $C_f = 0.01 \text{ m s}^{-1/2}$ and D_f is the characteristic of the leaves in the direction of the wind flow. The factor $(1/D_f)^{1/2}$ for each type of vegetation is given in BATS.

c) The balance of moisture of the foliage air layer

The balance of moisture of the foliage air layer assumes that the water vapor flux from the foliage air layer to the atmosphere (E_b) is equal to the sum of water vapor flux from the foliage to the foliage air layer (E_f) and water vapor flux from ground to the foliage air layer (E_g):

$$E_b = E_f + E_g \quad (11)$$

The parameterizations of E_f e E_g are similar to those given in BATS:

$$E_f = r'' E_f^{WET} \quad (12)$$

$$E_g = h f_g \rho_a c_p (q_{gs} - q_{af}) / c_p \quad (13)$$

where

$$E_f^{WET} = A_f (q_{fs} - q_{af}) \rho_a / r_{la} \quad (14)$$

and

$$r'' = 1 - \delta(E_f^{WET}) \{ 1 - L_w - L_d [r_{la} / (r_{la} + r_{stom})] \} \quad (15)$$

In the equations above, q_{fs} is the saturated mixing ratio at foliage temperature; A_f is the projected area of the wet surface ($\sigma_f L_{sai}$); $\delta(E_f^{WET})$ assumes the value 1 (if $\delta(E_f^{WET}) > 0$) or 0 (if $\delta(E_f^{WET}) \leq 0$); L_w and L_d are the fractional area of the leaves covered by water and the fraction of the foliage surface free to transpire, respectively, and are given by:

$$L_w = (W_{DW})^{2/3} \quad (16)$$

$$L_d = (1 - L_w) L_{AI} / L_{SAI} \quad (17)$$

where W_{DW} is a factor of interception of water that corresponds to the ratio between the total rainwater intercepted by the canopy (W_{dew}) and the maximum water the canopy can hold (W_{DMAX}).

The leaf-stem area index (L_{SAI}) is the sum of leaf area index (L_{AI}) and the stem area index (S_{AI}). The values of S_{AI} for each type of vegetation is given in BATS, and L_{AI} is expressed by:

$$L_{AI} = L_{AIN} + F_{sens}(T_{DL}) (L_{AIX} - L_{AIN}) \quad (18)$$

where the leaf area index minimum (L_{AIN}) and maximum (L_{AIX}) for each type of vegetation is given in BATS.

The stomatal resistance is parameterized like in BATS:

$$r_{stom} = r_{stomm} R_L S_L M_L \quad (19)$$

where the minimum stomatal resistance (r_{stomm}) for each vegetation type is given in BATS; R_L is a function of the solar radiation; S_L is the seasonal temperature factor, which is a function of the foliage temperature T_f ; and M_L is the soil moisture factor.

The expression for E_b proposed by Zhang (1994) is similar to that used by Saltzman & Vernekar (1971):

$$E_b = w [e_2 H_b(3) + f_2] / L \quad (20)$$

where $w = q_{af} / q_{afs}$, and q_{afs} is the saturated water vapor mixing ratio of the foliage air layer. The constants e_2 and f_2 are assumed equal to 2.4445 and 70.7827 J m⁻² s⁻¹, respectively. Although Eq. (20) is similar to that proposed by Saltzman & Vernekar (1971), there is a difference in the meaning of the variable w . Whereas in the model of Saltzman & Vernekar (1971) w is the water available parameter at surface, w in Zhang's biosphere model is the ratio q_{af} / q_{afs} , called relative humidity of the foliage air layer. As commented by Zhang (1994), this ratio has an important role in the partition of the surface net radiation into sensible and latent heat fluxes for mean annual and seasonally averaged conditions (because the subsurface flux is negligibly small in these cases). Since there are uncertainties in the determination of the water availability on land this substitution may not be adequate. Thus, Zhang (1994)

introduced a nondimensional adjustable factor Y for the relative humidity ($Y q_{af} / q_{afs}$). In the present work, we made sensitivity tests with respect to different values of Y .

Eq. (16) implies that the evaporation of water by the part of vegetation that is predominantly porous occurs like that at a liquid surface and not like that at a wet porous surface. Then, a factor ζ ($0 < \zeta \leq 1$) is introduced in this equation in order to consider the resistance to evaporation due to this part of vegetation. Sensitivity tests with respect to different values of ζ are given in the next section.

Regarding Eq. (11), note that :

$$H_b(4) = L E_b \quad (21)$$

and

$$L E_g = - H_s(4) \quad (22)$$

d) The energy balance of the foliage

The energy balance of the foliage assumes that the net radiation absorbed by the foliage (R_n) is balanced by the sensible (H_f) and latent ($L E_f$) heat fluxes from the foliage to the foliage air layer:

$$R_n = H_f + L E_f \quad (23)$$

with

$$R_n = H_b(1) + H_b(2) \quad (24)$$

where $H_b(1)$ and $H_b(2)$ are given in Tab. 2.

e) The closed system of equations of the biosphere model

Substitution of the flux Eqs. (9), (11), (13), (20) and the flux formulations given in Tabs. 1 and 2 into Eqs. (1), (8), (11), and (22) implies in a closed system of equations for the computation of T_{sv} , T_f , T_{af} , and q_{af} . The method to solve this closed system of equations is described in Appendix A.

The land surface model uses as input variables: the subsurface temperature (T_{DL}), the wind speed at the anemometer level (V_a), the solar radiation flux incident at the top of the atmosphere (R_o), and the temperature at 500 hPa (T_2); the output fields are the surface fluxes of energy and water vapor, the ground surface temperature (T_{sv}), the foliage temperature (T_f), the foliage air layer temperature (T_{af}), and the water vapor mixing ratio of the foliage air layer (q_{af}).

When the land surface model is running decoupled from the atmospheric model all the input variables are prescribed. In this case, the coefficients Ψ_i given in Tab. A1 and the saturated water vapor mixing ratio are recalculated at each interaction. When the vegetation model is running coupled to the SDM, the wind speed and the

temperature at 500 hPa are obtained from the atmospheric model at each time step and the other input variables are prescribed. Also, the coefficients are recalculated at each interaction at each time step. Details regarding the coupling of the biosphere model described above with the SDM are given in Varejão-Silva et al. (1998).

$$\Psi_1 = 1/\varepsilon_a + 1/\varepsilon_s - 1$$

$$\Psi_2 = 1/\varepsilon_f + 1/\varepsilon_s - 1$$

$$\Psi_3 = \rho_a C_p C_D [(1 - \sigma_f) V_a + \sigma_f U_{af}]$$

$$\Psi_4 = \Psi_3 L f_g / C_p$$

$$\Psi_5 = -\Psi_4$$

$$\Psi_6 = 1/\varepsilon_a + 1/\varepsilon_f - 1$$

$$\Psi_7 = \sigma_f L_{SAI} \rho_a C_p / r_{la}$$

$$\Psi_8 = -\Psi_7 - \Psi_3 - b_2 (C_D/C_{D0})$$

$$\Psi_9 = (b_2 T_2 - c_2) (C_D/C_{D0})$$

$$\Psi_{10} = -(e_2 b_2 / L) (C_D/C_{D0})$$

$$\Psi_{11} = -\Psi_{12} - \Psi_{13}$$

$$\Psi_{12} = \Psi_3 f_g / C_p$$

$$\Psi_{13} = \{L_w + L_d [r_{la} / (r_{la} + r_{stom})]\} \Psi_7 / C_p$$

$$\Psi_{14} = -\Psi_{10} T_2 - (e_2 c_2 C_D/C_{D0} + f_2) / L$$

$$\Psi_{18} = -\sigma_f \sigma_B / \Psi_2$$

$$\Psi_{19} = \sigma_f \sigma_B (1 / \Psi_2 + 1 / \Psi_6)$$

$$\Psi_{20} = L \Psi_{13}$$

$$\Psi_{21} = -\sigma_f [\sigma_B v_1 T_2^4 / \Psi_6 + (1 - \chi) (1 - r_f) (1 - r_a) R_o]$$

$$\Psi_{22} = -\sigma_B [(1 - \sigma_f) / \Psi_1 + \sigma_f / \Psi_2]$$

$$\Psi_{23} = (1 - \sigma_f) (1 - \chi) (1 - r_f) (1 - r_a) R_o + \sigma_B (1 - \sigma_f) v_1 T_2^4 / \Psi_1 + k_v T_{DL}$$

$$\Psi_{24} = -\Psi_3 - k_v$$

SENSITIVITY TESTS

In this section the vegetation model is run forced by prescribed variables in order to perform sensitivity tests concerning the behaviour of model variables with respect to different prescribed model parameters and different vegetation types. For this purpose, two types of vegetation were considered: the evergreen broadleaf forest and short grass. The model parameters for these vegetation types are obtained from BATS and are described in Dickinson et al. (1986). The other constants and prescribed input variables are given in Tab. 3.

The model considers that the vegetation is uniformly distributed over the surface. Although there are many parameters in the biosphere model, the effects of the changes of the fractional area covered by the vegetation (σ_f) and the water availability at the earth's surface (f_g) on the model variables deserve special attention because the drag coefficient and the albedo are strongly related to σ_f and the sensible and latent heat fluxes are most sensitive

$\gamma = 0.95$	$C_r = 0.01 \text{ m s}^{-1/2}$	$\rho_a = 1.2 \text{ kg m}^{-3}$
$\zeta = 1$	$c_p = 1004.0 \text{ J kg}^{-1} \text{ K}^{-1}$	$R_o = 444.3 \text{ W m}^{-2}$
$v_1 = 1.29$	$e^2 = 2.4445$	$r_f = 0.2$
$\sigma_H = 5.67 \times 10^{-8} \text{ W m}^{-2} \text{ K}^{-4}$	$f_2 = 70.7827 \text{ W m}^{-2}$	$r_{stom} = 5000 \text{ s m}^{-1}$
$\chi = 0.24$	$k = 0.484 \text{ W m}^{-2} \text{ K}^{-1}$	$T_2 = 267.19 \text{ K}$
$\varepsilon_a = 0.95$	$k_{VK} = 0.4$	$T_{DL} = 292.3$
$b_2 = 4.03 \text{ W m}^{-2} \text{ K}^{-1}$	$L = 2.501 \times 10^6 \text{ J kg}^{-1}$	$V_w = 2.0 \text{ m s}^{-1}$
$c_2 = -115.0 \text{ W m}^{-2}$	$M_1 = 1.0$	$z_1 = 10.0 \text{ m}$
$C_{D0} = 0.003$	$r_a = 0.28$	$z_{oh} = 0.02 \text{ m}$

Table 3 - Parameters and constants used in the vegetation model.

Tabela 3 - Parâmetros e constantes usadas no modelo de vegetação.

Table A1 - Ψ_i coefficients in the expressions of the biosphere model.

Tabela A1 - Coeficientes Ψ_i nas expressões do modelo da biosfera.

to f_g . Thus, the model response to variations on albedo, surface roughness (and consequently aerodynamic conductance) and soil moisture can be inferred through variations on these two parameters. The variation of σ_f from zero to 1 is of particular interest because it represents the gradual transition from completely bare land to fully

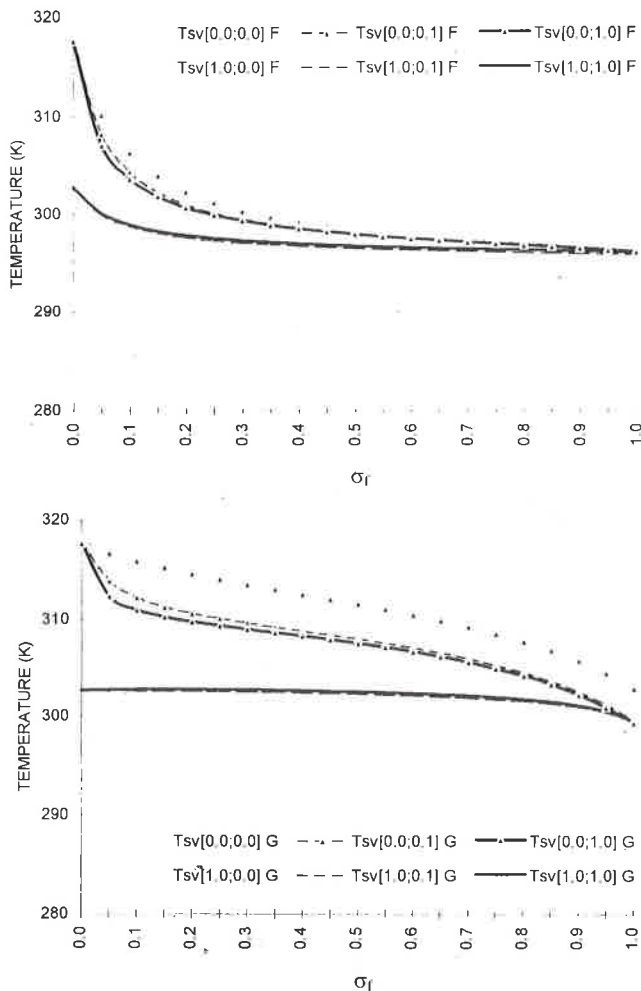


Figure 2 - Variation of the ground surface temperature (T_{sv}) with the fractional area of vegetation cover (σ_f), for different values of the water interception (W_{DW}) and the soil water availability (f_g). Legend: $T_{sv}(f_g, W_{DW}) X$, where $X=F$ for the case of forest (above) and $X=G$ for the case of short grass (below).

Figura 2 - Variação da temperatura da superfície do solo (T_{sv}) com a área fracional de cobertura vegetal (σ_f), para diferentes valores da interceptação de água (W_{DW}) e disponibilidade de água no solo (f_g). Legenda: $T_{sv}(f_g, W_{DW}) X$, onde $X=F$ para o caso de floresta (acima) e $X=G$ para o caso de pastagem (abaixo).

vegetation-covered ground so that both the effects of afforestation and degradation of the vegetation are taken into account.

Sensitivity tests concerning the effect of the change of σ_f on the variation of the temperatures (T_{sv} , T_f , T_{af}), the water vapor mixing ratio of the foliage air layer (q_{af}), and the fluxes of energy and water vapor are made considering different values of f_g (Figs. 2-10). Since the latent heat flux depends on the factor of interception of water (W_{DW}) the effects of its variation are also investigated. For these experiments the values of Y and ζ are assumed equal to 1.

Figs. 2-5 show the variation of the T_{sv} , T_f , and T_{af} with respect to σ_f , for different values of f_g and W_{DW} . As can be seen in Fig. 2, the maximum value of T_{sv} occurs when there is no vegetation ($\sigma_f = 0$). This value is higher for the lower values of f_g . In fact, when $f_g \neq 0$ a part of the solar radiation flux absorbed at the surface is used in the evaporation process and, consequently, T_{sv} cannot reach high values as in the case of bare land. For the same curve (f_g and W_{DW} are fixed values) T_{sv} decreases as the values of σ_f are larger. There is no evaporation both at ground surface and the foliage when $W_{DW} = f_g = 0$ and, consequently, T_{sv} is higher for each value of $\sigma_f \neq 0$. In the case that $\sigma_f \neq 0$, if $f_g \neq 0$ and $W_{DW} = 0$ more available energy will be used in the evaporation of the soil water causing a reduction in T_{sv} ; also, in the case $f_g \neq 0$, there is an increase in T_{sv} due to the increasing of W_{DW} (increase of the evaporation of the intercepted water) because the wet foliage air layer difficults the evaporation of the soil water. Finally, in the same conditions of f_g , W_{DW} , and σ_f , T_{sv} is higher in the evergreen broadleaf forest than in the short grass due to the surface roughness effect. Also, the results indicate that T_{sv} is almost independent on the values of $W_{DW} > 0.2$ (not shown).

Fig. 3 shows the variation of T_f with σ_f . As can be noted, in both the evergreen broadleaf forest and short grass, when there is no interception ($W_{DW} = 0$) and the ground is dry ($f_g = 0$) T_f decreases as σ_f increases because the energy consumption in the transpiration process overcomes the gain of shortwave solar radiation caused by the reduction of the albedo. When the ground is dry ($f_g = 0$), but there is evaporation of the intercepted water by the foliage ($W_{DW} \neq 0$), the values of T_f increase progressively with the increase in σ_f ($\sigma_f > 0.5$). This indicates that the moistening of the foliage air layer caused by the evaporation of the intercepted water tends to inhibit the transpiration process and,

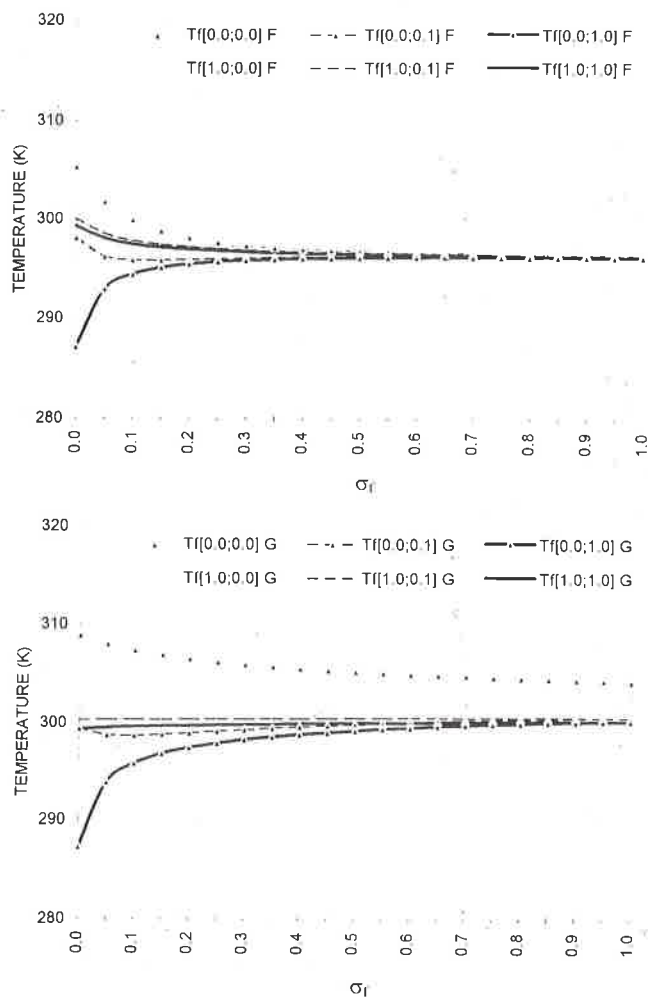


Figure 3 - The same as in Fig. 2, but for the foliage temperature (T_f).

Figura 3 - O mesmo que a Fig. 2, mas para a temperatura da folhagem (T_f).

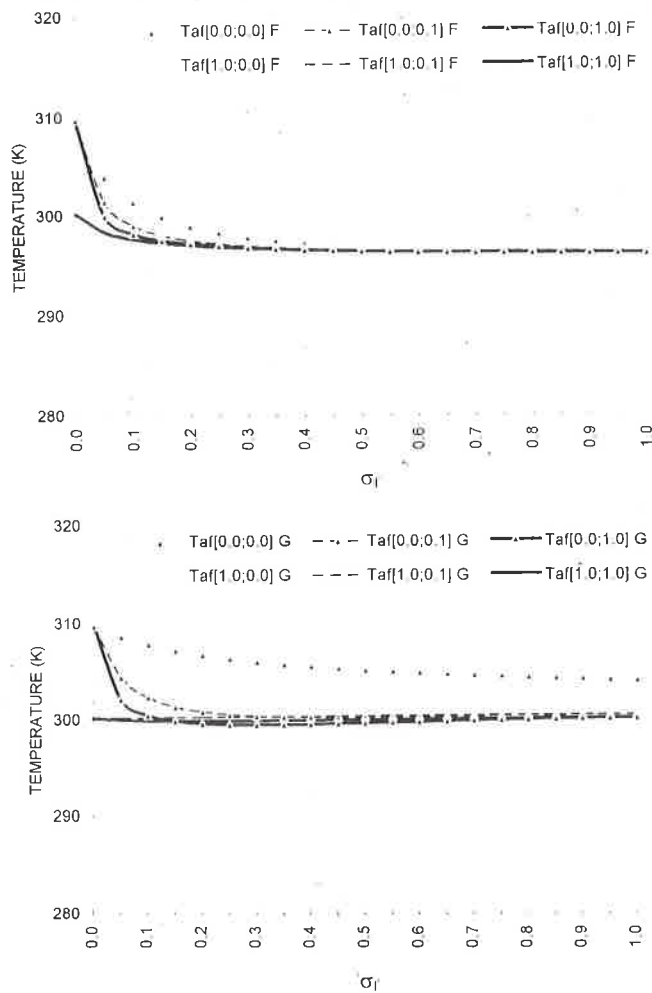


Figure 4 - The same as in Fig. 2, but for the foliage air layer temperature (T_{af}).

Figura 4 - O mesmo que a Fig. 2, mas para a temperatura da camada de ar na folhagem (T_{af}).

consequently, making more energy available as sensible heat flux at the surface foliage. Finally, if there are both water availability at ground ($f_g \neq 0$) and interception ($W_{DW} \neq 0$) the transpiration is progressively reduced as W_{DW} increases, so that the variation of T_f becomes very small for large values of σ_f . As can be seen, T_f is practically insensitive to the variations of f_g and W_{DW} (when they are not equal to zero) for $\sigma_f \geq 0.7$. This behaviour is a result of the fact that the evaporation of the intercepted water is a dominant component of the evapotranspiration in these conditions (as it will be seen later) and the transpiration is substantially reduced.

The variation of T_{af} with σ_f for different values of f_g and W_{DW} is presented in Fig. 4. In general, the variation of T_{af} is similar to that of T_f . This is better illustrated in Fig. 5, where the simultaneous variation of T_{sv} , T_f , and T_{af} considering two different interceptions ($W_{DW} = 0$ and $W_{DW} = 0.1$) for a fixed value of $f_g (= 0.5)$ are shown. In the case of the evergreen broadleaf forest, when $W_{DW} = 0$ the values of T_f are higher than those of T_{af} . Both values of T_f and T_{af} decrease monotonically tending to the same value. T_{sv} is higher than T_f and T_{af} for low values of σ_f . However, when $\sigma_f > 0.3$ the values of T_{sv} are lower than those from the other two temperatures because the foliage shades the

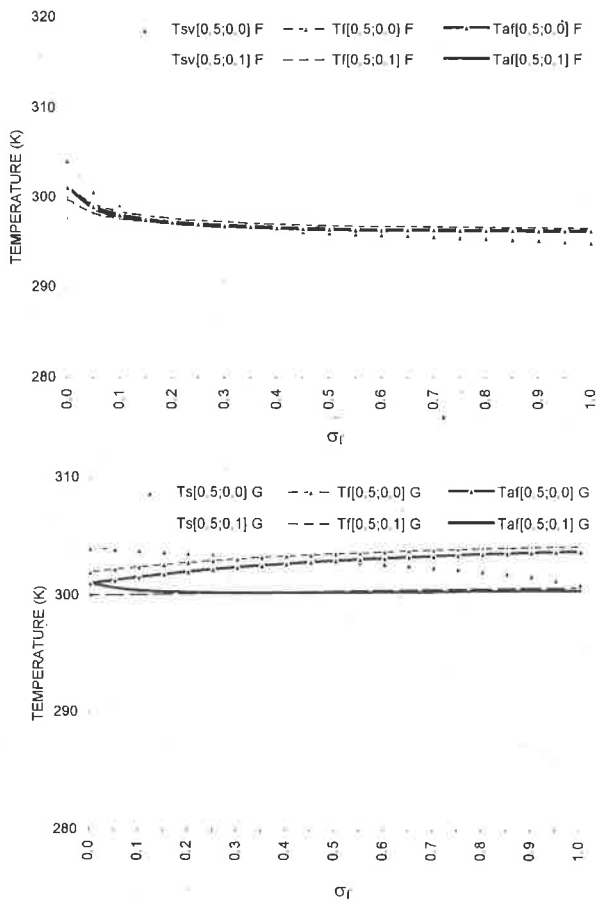


Figure 5 - Variation of the ground surface temperature (T_{sv}), the foliage temperature (T_f) and the foliage air layer temperature (T_{af}) with the fractional area of vegetation cover (σ_f), for $f_b=0.5$ and different values of W_{DW} , in the case of forest and short grass. Legend: similar to Fig. 2.

Figura 5 - Variação das temperaturas da superfície do solo (T_{sv}) e da camada de ar na folhagem (T_{af}) com a área fracional de cobertura vegetal (σ_f), para $f_b = 0,5$ e diferentes valores de W_{DW} , para o caso de floresta perenifolia e pastagem. Legenda similar à da Fig. 2.

ground. When there is interception ($W_{DW} = 0.1$) $T_{af} > T_f$ due to the evaporation of the intercepted water and also to the influence of the soil surface without vegetation (approximately for $\sigma_f < 0.25$). The reduction of T_{sv} with the increase of the vegetation cover cause a cooling of foliage air layer making $T_{af} < T_f$ for $\sigma_f > 0.25$. In the case of short grass, when there is no interception ($W_{DW} = 0$) T_f is

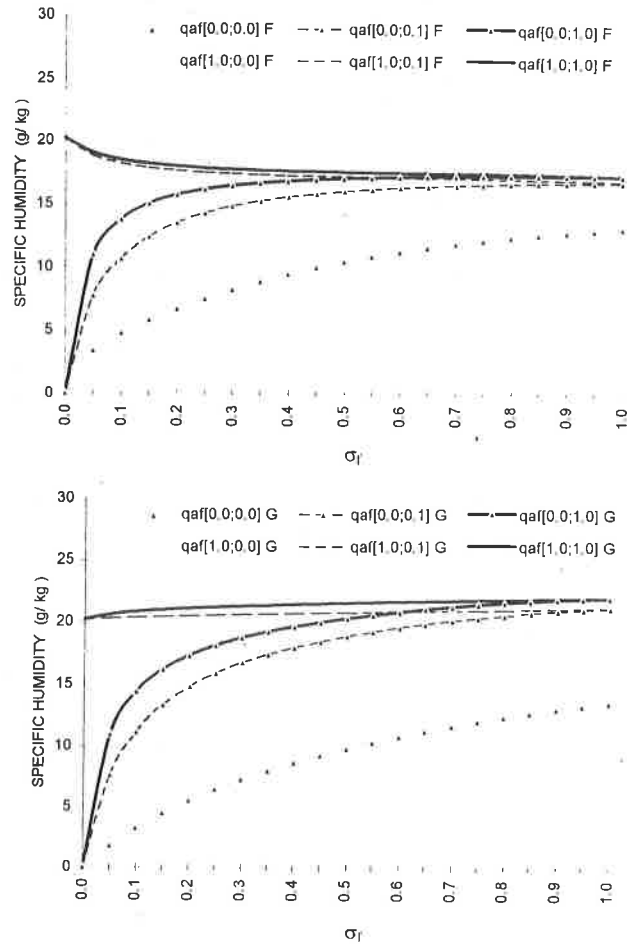


Figure 6 - The same as in Fig. 2, but for the water vapor mixing ratio in the foliage air layer (q_{af}).

Figura 6 - O mesmo que a Fig. 2, mas para a razão de mistura do vapor d'água na camada de ar na folhagem (q_{af}).

always higher than T_{nf} even in the situation of the shading of ground (increase of σ_f). When there is interception it is noted that $T_f < T_{af}$ for $\sigma_f > 0.4$ and the difference between these temperatures increases slightly with σ_f . The stem area index (S_{AI}) is greater in short grass than in evergreen broadleaf forest. Although this material is biologically inactive, it intercepts water and influences in the energy and moisture balances and, consequently, together with the other vegetation specific parameters, it also contributes to the different behaviour of T_{sv} , T_f and T_{af} in the cases of forest and grassland.

Fig. 6 shows the variation of the water vapor mixing

ratio of the foliage layer (q_{af}) with σ_f . When the ground is dry ($f_g=0$) q_{af} increases with σ_f due to only the transpiration (if $W_{DW}=0$) and also to the transpiration together with the evaporation of intercepted water (if $W_{DW}\neq 0$), in both the cases of evergreen broadleaf forest and short grass. For a fixed value of σ_f there is an increase of q_{af} with the increasing of the evaporation of either the water at soil surface or the water intercepted by the foliage. However,

when $f_g \neq 0$ (wet soil) and $W_{DW}=0$ (no water interception) q_{af} decreases as σ_f tends to unity because the expansion of the fractional area of the vegetation cover reduces solar radiation incident at the ground surface and, consequently, the evaporation process. The difference between the results for the two types of vegetation occurs in the case of large interception and high soil moisture. In this situation, as σ_f increases the water vapor flux from foliage becomes the dominant component and tends to moist excessively the foliage air layer. This causes a large decrease in the evaporation of water at the ground surface and also in the transpiration. Since the drag coefficient is larger in the forest than in the short grass the transference of water vapor to the atmosphere is more efficient and, consequently, there is a decrease of the foliage air layer moisture. So, q_{af} decreases as σ_f is larger. In the case of short grass, as the drag coefficient is too much smaller than that of the forest, q_{af} increases monotonically with σ_f when f_g and W_{DW} are larger enough.

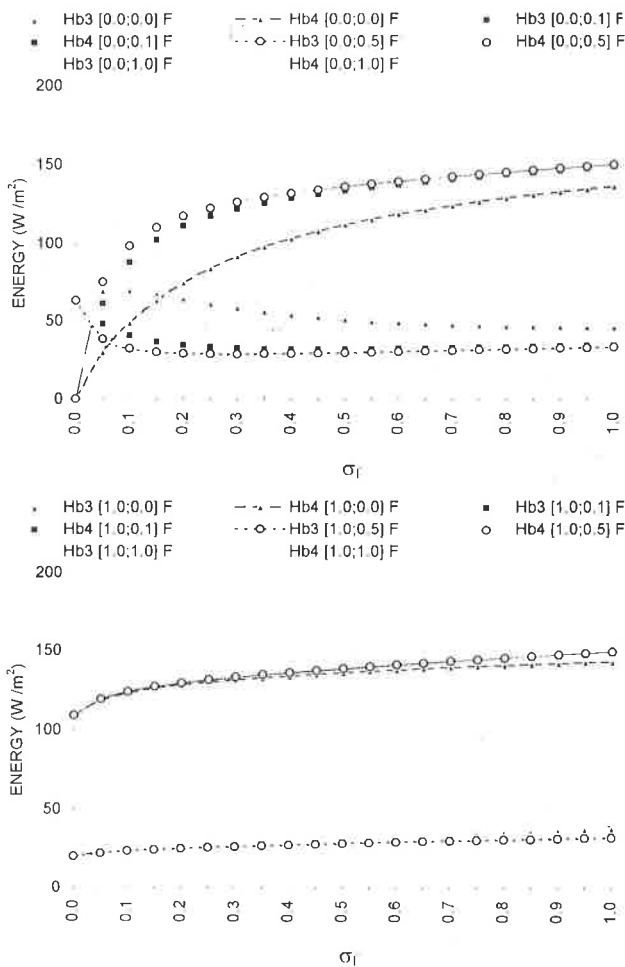


Figure 7 - Variation of the sensible [$H_b(3)$] and latent [$H_b(4)$] heat fluxes with the fractional area of vegetation cover (σ_f) for the dry soil ($f_g=0$) (above) and fully water soil ($f_g=1.0$) (below) and different values of interception (W_{DW}) in the case of forest. Legend: similar to Fig. 2.

Figura 7 - Variação dos fluxos de calor sensível [$H_b(3)$] e latente [$H_b(4)$] com a área fracional de cobertura vegetal (σ_f), para solo seco ($f_g = 0,0$) (acima) e completamente molhado ($f_g = 1,0$) (abaixo) e diferentes valores de interceptação (W_{DW}) no caso de floresta perenifolia. Legenda similar à da Fig. 2.

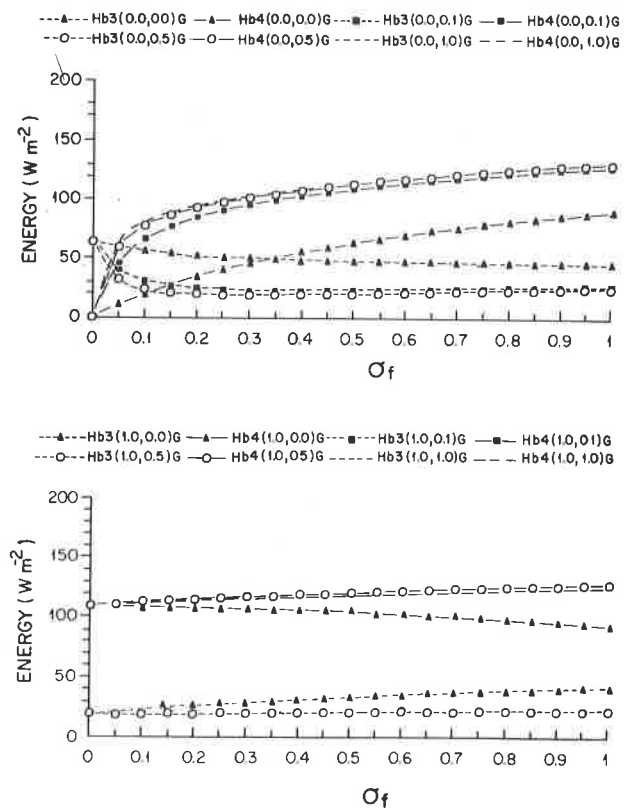


Figure 8 - the same as in Fig. 7, but for the case of short grass.

Figura 8 - O mesmo que a Fig. 7, mas para o caso de pastagem.

The variation of the sensible $[(H_b(3))]$ and latent $[(H_b(4))]$ heat fluxes with respect to σ_f is shown in Figs. 7 and 8 for the cases of evergreen broadleaf forest and short grass, respectively. When the ground is dry ($f_g = 0$) the sensible and latent heat fluxes to the atmosphere only depend on the intercepted water by the foliage and on the transpiration. The values of $H_b(4)$ increase as σ_f is also increased, while the $H_b(3)$ values are reduced. Evidently, the latent heat flux is larger as the interception (W_{DW}) increases for both the cases of forest and short grass. Also, for these vegetation types, the dependency of sensible and latent heat fluxes on σ_f is significative only for $W_{DW} < 0.2$. For higher values of W_{DM} the sensible and latent heat fluxes become almost independent of the interception, mainly for larger values of σ_f . When the interception ($W_{DW} = 1$) is maximum, as the entire foliage surface is wet the transpiration process is stopped and the foliage air layer becomes saturated. Then, the evaporation of the water at the soil surface occurs only in the fractional area not covered

by the vegetation ($1 - \sigma_f$). Since the soil surface is wet ($f_g \neq 0$), if the interception is not maximum ($W_{DW} < 1$), part of the available energy is used in the evaporation of the water at the ground surface. In these conditions, for a given value of σ_f the sensible heat flux to the atmosphere decreases with the increase of f_g . The opposite occurs with the latent heat flux.

Since the subsurface conduction flux is small, the available energy (AE) at the surface is divided into sensible and heat fluxes. So, it can be assumed that $AE \cong H_b(3) + H_b(4)$. The variation of the available energy with respect to σ_f considering the cases of evergreen broadleaf forest and short grass is showed in Figs. 9 and 10, respectively. In these figures, the situations of dry soil ($f_g = 0$) and fully water saturated ground ($f_g = 1$) are analysed considering different values of the interception. The results show that

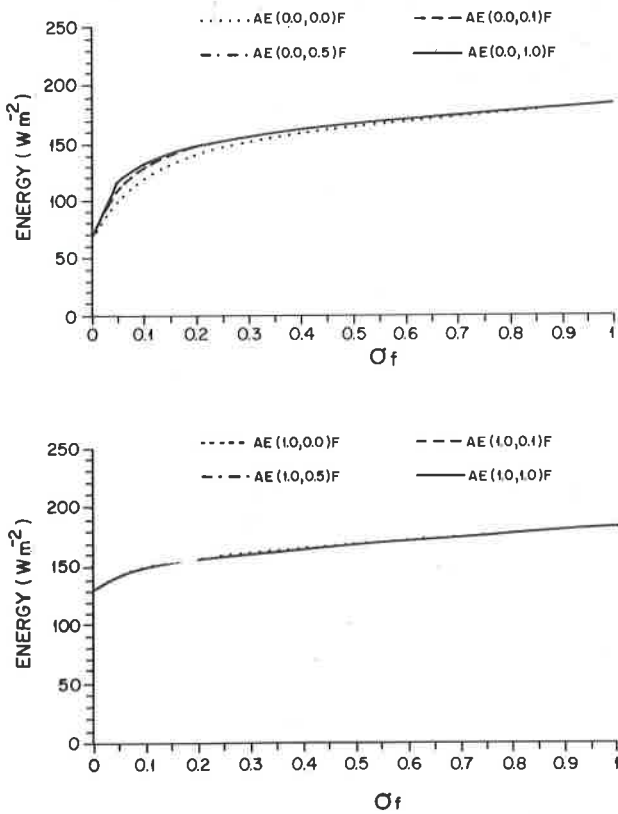


Figure 9 - The same as in Fig. 7, but for the available energy at surface.

Figura 9 - O mesmo que a Fig. 7, mas para a energia disponível na superfície.

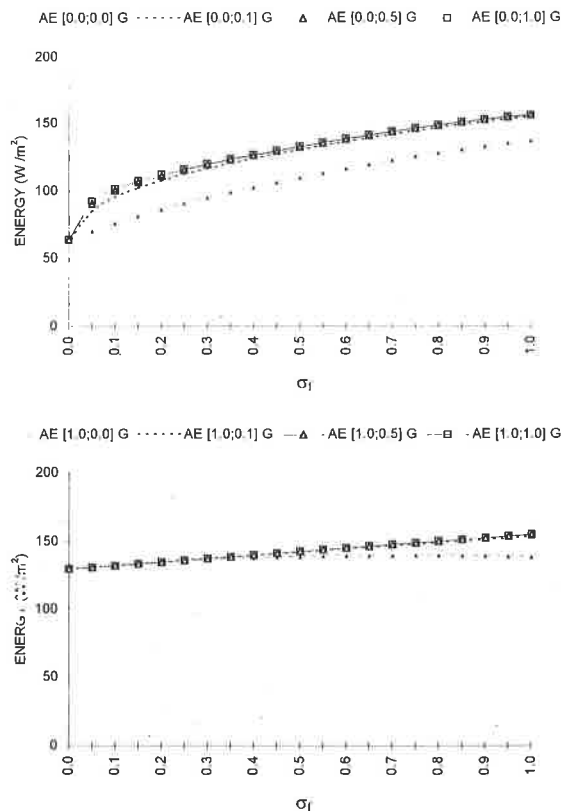


Figure 10 - The same as in Fig. 8, but for the available energy at surface.

Figura 10 - O mesmo que a Fig. 8, mas para a energia disponível na superfície.

in the case of dry soil, for both the vegetation types, AE increases with the increase in σ_f . This is because the latent heat flux increases quickly with σ_f while the decrease of the sensible heat flux is slow. Also, in this situation the variation of AE is almost insensitive for $W_{DW} > 0.2$, mainly when σ_f is larger. In the case of fully wet soil the dependency of the available energy on the interception is reduced. This is physically consistent because the evaporation at the soil surface increases the latent heat flux to the atmosphere, even when the interception is small or nil. Evidently, the effect of the soil water availability is reduced with the increase of W_{DW} and σ_f because the water vapor flux due to the wet foliage evaporation tends to moisten quickly the foliage air layer and, consequently, prevents the evaporation from the soil surface.

As mentioned before, a factor ζ was inserted in Eq. (16) to take into account the resistance to evaporation due to the part of vegetation which is predominantly porous. Tabs. 4 and 5 show the variation of the component terms of the evapotranspiration with respect to ζ (for $Y = 1$). For $\zeta = 1$, although the values of interception are low the transpiration is practically stopped (see, for example, the case $W_{DW} = 0.1$). This behaviour is physically inconsistent and it is due to the fact that the evaporation of the intercepted water is dominant in the model parameterization. Considering the case $\delta(E_f^{WET}) = 1$, it can be obtained from Eqs. (14) and (15):

$$E_f = \sigma_f L_{sai} \rho_a A_f (q_{fs} - q_{af}) L_w / r_{la} + \sigma_f L_{sai} \rho_a (q_{fs} - q_{af}) L_d / (r_{la} + r_{stom}) \quad (36)$$

where the first and the second right term represent the contribution of the intercepted water (E_w) and the transpiration (E_t), respectively. This formulation considers that the stem water interception evaporates (like a thin skin) with no resistance of the substrate that involves this part of vegetation (note that only $1/r_{la}$ is included in the term which represents E_w). This is correct during and just after the occurrence of precipitation. In fact, a fraction of the intercepted water is absorbed by the part of vegetation predominantly porous, which is constituted by leaves on the ground, stem, and even falling branches of trees covered by porous material, which are in different stages of decomposition. These materials prevent evaporation of the absorbed water which is not taken into account in the original model parameterization. Then, in the present work, a factor ζ ($0 < \zeta < 1$) is inserted in Eq. (16) in order to simulate

$\zeta = 1.0; Y = 1.0$									
σ_f	$f_g = 0.0; W_{DW} = 0.0$			$f_g = 0.0; W_{DW} = 0.1$			$f_g = 0.0; W_{DW} = 1.0$		
	E_w	E_{tr}	E_g	E_w	E_{tr}	E_g	E_w	E_{tr}	E_g
0.2	0.00	0.26	0.00	0.33	0.06	0.00	0.41	0.00	0.00
0.6	0.00	0.41	0.00	0.41	0.06	0.00	0.48	0.00	0.00
1.0	0.00	0.47	0.00	0.45	0.06	0.00	0.52	0.00	0.00
σ_f	$f_g = 1.0; W_{DW} = 0.0$			$f_g = 1.0; W_{DW} = 0.1$			$f_g = 1.0; W_{DW} = 1.0$		
	E_w	E_{tr}	E_g	E_w	E_{tr}	E_g	E_w	E_{tr}	E_g
0.2	0.00	0.04	0.40	0.08	0.01	0.35	0.13	0.00	0.32
0.6	0.00	0.13	0.35	0.24	0.03	0.21	0.32	0.00	0.16
1.0	0.00	0.27	0.22	0.42	0.05	0.05	0.51	0.00	0.00
$\zeta = 0.2; Y = 1.0$									
σ_f	$f_g = 0.0; W_{DW} = 0.0$			$f_g = 0.0; W_{DW} = 0.1$			$f_g = 0.0; W_{DW} = 1.0$		
	E_w	E_{tr}	E_g	E_w	E_{tr}	E_g	E_w	E_{tr}	E_g
0.2	0.00	0.26	0.00	0.15	0.17	0.00	0.32	0.06	0.00
0.6	0.00	0.41	0.00	0.24	0.21	0.00	0.41	0.06	0.00
1.0	0.00	0.47	0.00	0.28	0.22	0.00	0.45	0.06	0.00
σ_f	$f_g = 1.0; W_{DW} = 0.0$			$f_g = 1.0; W_{DW} = 0.1$			$f_g = 1.0; W_{DW} = 1.0$		
	E_w	E_{tr}	E_g	E_w	E_{tr}	E_g	E_w	E_{tr}	E_g
0.2	0.00	0.04	0.40	0.03	0.03	0.39	0.08	0.02	0.35
0.6	0.00	0.13	0.35	0.10	0.09	0.29	0.23	0.04	0.20
1.0	0.00	0.27	0.22	0.21	0.16	0.13	0.41	0.06	0.49
$\zeta = 0.1; Y = 1.0$									
σ_f	$f_g = 0.0; W_{DW} = 0.0$			$f_g = 0.0; W_{DW} = 0.1$			$f_g = 0.0; W_{DW} = 1.0$		
	E_w	E_{tr}	E_g	E_w	E_{tr}	E_g	E_w	E_{tr}	E_g
0.2	0.00	0.26	0.00	0.09	0.20	0.00	0.25	0.11	0.00
0.6	0.00	0.41	0.00	0.16	0.28	0.00	0.34	0.12	0.00
1.0	0.00	0.47	0.00	0.19	0.30	0.00	0.38	0.12	0.00
σ_f	$f_g = 1.0; W_{DW} = 0.0$			$f_g = 1.0; W_{DW} = 0.1$			$f_g = 1.0; W_{DW} = 1.0$		
	E_w	E_{tr}	E_g	E_w	E_{tr}	E_g	E_w	E_{tr}	E_g
0.2	0.00	0.04	0.40	0.02	0.04	0.39	0.05	0.02	0.37
0.6	0.00	0.13	0.35	0.06	0.10	0.32	0.17	0.06	0.25
1.0	0.00	0.27	0.22	0.13	0.20	0.17	0.32	0.10	0.08

Table 4 - Computation of the evapotranspiration terms considering different values of the interception (W_{DW}) and soil water availability (f_g) for the case of evergreen broadleaf forest: (a) $\zeta=1.0$ and $Y=1.0$; (b) $\zeta=0.2$ and $Y=1.0$; and (c) $\zeta=0.1$ and $Y=1.0$. E_w , E_{tr} , and E_g are the evaporation of the intercepted water, the transpiration, and the soil water evaporation, respectively.

Tabela 4 - Cálculo dos termos da evapotranspiração considerando diferentes valores da interceptação (W_{DW}) e disponibilidade de água no solo (f_g) para o caso de floresta perenifólia: a) $\zeta = 1,0$ e $Y = 1,0$; b) $\zeta = 0,2$ e $Y = 1,0$; e c) $\zeta = 0,1$ e $Y = 1,0$. E_w , E_{tr} e E_g correspondem à evaporação de água interceptada, transpiração e evaporação de água da superfície do solo, respectivamente.

this effect. As can be seen in Tabs. 4 and 5, better results are obtained for small values of ζ . However, it must be noted that for a given combination of (f_g, W_{DW}) , for the same prescribed parameters and input data, the total flux of water vapor to the atmosphere (evapotranspiration) does not change with ζ and, consequently, the latent heat flux to the atmosphere is independent of the evapotranspiration partitioning into its components. In fact, it is noted from Eqs. (20) and (21) that the evapotranspiration (E_e) is proportional

to the latent heat flux [$H_b(4)$], which in turn is proportional to the sensible heat flux. The weak dependency of the evapotranspiration on the variation of ζ is noted in Tabs. 4 and 5.

Another sensitivity test was made considering the behaviour of the model variables with respect to the variations of the nondimensional adjustable factor (Y) introduced in Eq. (20), as mentioned in a previous section. As can be noted in Fig. 11, this factor modifies the latent heat flux to the atmosphere and, consequently, the total flux of the available energy at the surface. The effect of Y consists in the adjustment of the partitioning of the available radiation into latent and sensible heat fluxes. The use of Y

$\zeta = 1.0; Y = 1.0$									
σ_f	$f_r = 0.0; W_{DW} = 0.0$			$f_r = 0.0; W_{DW} = 0.1$			$f_r = 0.0; W_{DW} = 1.0$		
	E_w	E_{tr}	E_r	E_w	E_{tr}	E_r	E_w	E_{tr}	E_r
0.2	0.00	0.12	0.00	0.27	0.02	0.00	0.32	0.00	0.00
0.6	0.00	0.24	0.00	0.36	0.02	0.00	0.40	0.00	0.00
1.0	0.00	0.31	0.00	0.41	0.03	0.00	0.45	0.00	0.00
σ_f	$f_r = 1.0; W_{DW} = 0.0$			$f_r = 1.0; W_{DW} = 0.1$			$f_r = 1.0; W_{DW} = 1.0$		
	E_w	E_{tr}	E_r	E_w	E_{tr}	E_r	E_w	E_{tr}	E_r
0.2	0.00	0.03	0.35	0.09	0.01	0.30	0.12	0.00	0.28
0.6	0.00	0.13	0.23	0.26	0.02	0.14	0.30	0.00	0.12
1.0	0.00	0.29	0.04	0.41	0.03	0.00	0.45	0.00	0.00
$\zeta = 0.2; Y = 1.0$									
σ_f	$f_r = 0.0; W_{DW} = 0.0$			$f_r = 0.0; W_{DW} = 0.1$			$f_r = 0.0; W_{DW} = 1.0$		
	E_w	E_{tr}	E_r	E_w	E_{tr}	E_r	E_w	E_{tr}	E_r
0.2	0.00	0.12	0.00	0.14	0.06	0.00	0.26	0.02	0.00
0.6	0.00	0.24	0.00	0.24	0.10	0.00	0.36	0.03	0.00
1.0	0.00	0.31	0.00	0.28	0.12	0.00	0.41	0.03	0.00
σ_f	$f_r = 1.0; W_{DW} = 0.0$			$f_r = 1.0; W_{DW} = 0.1$			$f_r = 1.0; W_{DW} = 1.0$		
	E_w	E_{tr}	E_r	E_w	E_{tr}	E_r	E_w	E_{tr}	E_r
0.2	0.00	0.03	0.35	0.04	0.02	0.32	0.09	0.01	0.30
0.6	0.00	0.13	0.23	0.15	0.06	0.17	0.26	0.02	0.14
1.0	0.00	0.29	0.04	0.28	0.11	0.02	0.41	0.03	0.02
$\zeta = 0.1; Y = 1.0$									
σ_f	$f_r = 0.0; W_{DW} = 0.0$			$f_r = 0.0; W_{DW} = 0.1$			$f_r = 0.0; W_{DW} = 1.0$		
	E_w	E_{tr}	E_r	E_w	E_{tr}	E_r	E_w	E_{tr}	E_r
0.2	0.00	0.12	0.00	0.09	0.08	0.00	0.22	0.04	0.00
0.6	0.00	0.24	0.00	0.16	0.14	0.00	0.32	0.05	0.00
1.0	0.00	0.31	0.00	0.20	0.17	0.00	0.36	0.06	0.00
σ_f	$f_r = 1.0; W_{DW} = 0.0$			$f_r = 1.0; W_{DW} = 0.1$			$f_r = 1.0; W_{DW} = 1.0$		
	E_w	E_{tr}	E_r	E_w	E_{tr}	E_r	E_w	E_{tr}	E_r
0.2	0.00	0.03	0.35	0.02	0.02	0.33	0.07	0.01	0.31
0.6	0.00	0.13	0.23	0.10	0.08	0.19	0.22	0.04	0.15
1.0	0.00	0.29	0.04	0.19	0.16	0.02	0.36	0.06	0.07

Table 5 - The same as in Tab. 4 but for short grass.

Tabela 5 - O mesmo que a Tab. 4, mas para pastagem.

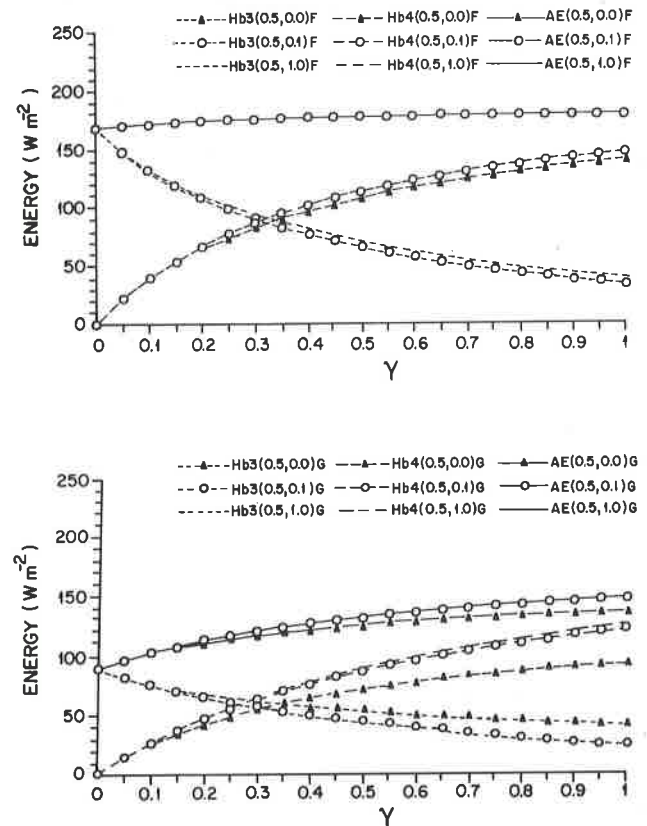


Figure 11 - Variation of the available energy at the surface with the adjustable factor Y , for different values of the interception (W_{DW}) and $f_g=0.5$, for the cases of forest (above) and short grass (below). Legend: similar to Fig. 2.

Figura 11 - Variação da energia disponível na superfície com o fator de ajuste Y , para diferentes valores de interceptação (W_{DW}) e $f_g = 0,5$, para os casos de floresta perenifolia (acima) e pastagem (abaixo). Legenda similar à da Fig. 2.

compensates partially the fact that there is not a soil hydrology parameterization in the model. It should be borne in mind that although Y modifies the Bowen ratio it does not change the partitioning of the evapotranspiration into its component terms. In other words, the proportion between the interception, transpiration and the evaporation from the ground is maintained.

Fig. 11 shows the variation of the energy fluxes with respect to Y for the situation where $\zeta = 1$, $f_g = 0.5$, and the interception is varying ($W_{DW} = 0, 0.1, 1$) considering the cases of evergreen broadleaf forest and short grass. As can be seen, the sensible heat flux to the atmosphere increases progressively with the decrease of Y in both vegetation types. The opposite occurs with the latent heat flux. $H_b(3)$ and $H_b(4)$ are approximately equal when $Y = 0.3$. For a given value of Y , the model is almost insensitive to high values of W_{DW} . This is due to the fact that when $W_{DW} > 2$ the evaporation from the intercepted water by the foliage and the part of vegetation predominantly porous becomes the dominant component of the water vapor flux to the atmosphere.

SUMMARY AND CONCLUSIONS

A biosphere model based on BATS adapted to the energy flux formulations of a SDM is described. The vegetation model is used to perform sensitivity tests concerning the behaviour of the model variables with respect to different prescribed model parameters and contrasting vegetation types, such as evergreen broadleaf forest and short grass.

The results show that the ground surface temperature decreases with the increase in the fractional area of the vegetation cover due to the lower solar radiation flux absorbed at surface in both the vegetation types. In the case of the wet soil surface, the ground surface temperature increases with the increase in the interception because the wet foliage air layer difficulties the evaporation of the soil water. The values of the ground surface temperature are almost independent for $W_{DW} > 0.2$, where W_{DW} is the ratio between the total rainwater intercepted by the canopy and the capacity of the canopy to intercept rainwater. Also, the soil surface temperature is lower in the forest than in the short grass due to the surface roughness effect.

When the soil is dry, and if there is interception, the foliage temperature increases with the increase of the

fractional area of the vegetation cover for both the forest and grassland cases. This is due to the fact that the moistening of the foliage air layer caused by the intercepted water prevents the transpiration process, making more available energy as sensible heat flux at the foliage surface. In the case of wet soil the transpiration is reduced with the increase of the interception, so that the variation of the foliage temperature is very small for large values of the fractional area of the vegetation cover. In general, the behaviour of the foliage air temperature is similar to the foliage temperature.

Regarding the water vapor mixing ratio, the largest difference between the results for forest and grassland occurs when there are large interception and high soil moisture. In this case, as the fractional area of the vegetation cover is increased, the water vapor flux from foliage becomes the dominant component and tends to excessively moisten the foliage air layer. Consequently, there is a large decrease in both the ground surface evaporation and transpiration. Since the drag coefficient is larger in the forest than in the short grass the transference of water vapor to the atmosphere is more efficient, so that there is a decrease in the foliage air layer moisture. Otherwise, since the drag coefficient of the short grass is small the water vapor mixing ratio increases monotonically with the fractional area of the vegetation cover for larger enough values of the soil water availability and interception.

In both vegetation types, when the soil is dry the available energy increases with increase in the fractional area of the vegetation due to the fact that the latent heat flux increases quickly with σ_f while the sensible heat flux decreases slowly. Also, the available energy is almost insensitive to values of $W_{DW} > 0.2$. In the case of the saturated wet soil the available energy dependency on the interception is reduced because the water evaporation at the ground surface increases the latent heat flux, even if the interception is small or null.

Sensitivity tests were made regarding the factor ζ , which was inserted in Eq. (16) (relation which gives the fractional area of the leaves covered by water) to take into account the effect of the resistance to the evaporation due to the predominantly porous part of the vegetation. The case $\zeta = 1$, as used by Zhang (1994), produces physically inconsistent results regarding the evapotranspiration component terms: for low values of the interception the transpiration process is practically ceased. This behaviour is due to the fact that the

evaporation of the intercepted water is the dominant component in the evapotranspiration according to the parameterization used in the model. The original formulation assumes that the stem water interception evaporates with no resistance of the substrate that involves it. However, a fraction of the intercepted water is absorbed by the predominantly porous part of the vegetation (leaves on the ground, stem and falling branches of trees). The resistance to the absorbed water due to this part of the vegetation is not taken into account in the original parameterization. Thus, the formulation of the evapotranspiration must be improved in order to study the partitioning into interception, evaporation at the ground surface, and transpiration. The values $\zeta < 1$ are tested with the purpose of simulating the effect of the resistance of the porous part of vegetation. The results show that the better results concerning the component terms of evapotranspiration are obtained with small values of ζ . However, the total flux of water vapor to the atmosphere does not change with ζ and, consequently, the latent heat flux to the atmosphere doesn't depend on the partitioning of the evapotranspiration into its component terms.

Sensitivity tests were made with respect to the adjustable factor Y introduced in Eq. (20) (relation that gives the water vapor flux to the atmosphere). The effect of Y consists in the adjustment of the partitioning of the available radiation into latent and sensible heat and its use compensates partially the fact that there is not a soil hydrology parameterization in the model. The results show that the latent heat flux increases with the increase of Y and the opposite occurs with the sensible heat flux. These fluxes are approximately equal for $Y = 0.3$. It is interesting to note that, although the variation of Y modifies the Bowen ratio, it does not change the evapotranspiration partitioning into its component terms.

REFERENCES

- BUDYKO, M. I. - 1982** - The Earth's climate: past and future. Academic Press, 307 pp.
- DICKINSON, R. E., HENDERSON-SELLERS, A., KENNEDY, P. J. & WILSON, M. F. - 1986** - Biosphere-Atmosphere Transfer Scheme for the NCAR Community Climate Model. NCAR, Tech. Note 275+STR, 69 pp.
- DICKINSON, R. E. & HENDERSON-SELLERS, A. - 1988** - Modeling tropical deforestation: a study of GCM land surface parameterizations. Quarterly Journal of the Royal Meteorological Society, **114**: 439-462.
- DIRMEYER, P. A. & SHUKLA, J. - 1994** - Albedo as modulator of climate response to tropical deforestation. Journal of Geophysical Research, **99(D10)**: 20863-20877.
- FRANCHITO, S. H. & RAO, V. B. - 1992** - Climatic change due to land surface alterations. Climatic Change, **22**: 1-34.
- GUTMAN, G., OHRING G. & JOSEPH, J. H. - 1984** - Interaction between the geobotanic state and climate: a suggested approach and test with a zonal model. Journal of the Atmospheric Sciences, **41**: 2663-2677.
- HENDERSON-SELLERS, A., DICKINSON, R. E., DURBIDGE, T. B., KENNEDY, P. J., MCGUFFIE, K. M. & PITMAN, A. J. - 1993** - Tropical deforestation: modeling local- to regional-scale climate change. Journal of Geophysical Research, **98(D4)**: 7289-7315.
- NOBRE, C. A., SELLERS, P. J. & SHUKLA, J. - 1991** - Amazonian deforestation and regional climate change. Journal of Climate, **4**: 957-987.
- NOILHAN, J. & PLANTON, S. - 1989** - A simple parameterization of land surface processes for meteorological models. Monthly Weather Review, **117**: 536-549.
- SAGAN, C., TOM, O. B. & POLLACK, J. B. - 1979** - Anthropogenic albedo changes and the earth's climate. Science, **206**: 1363-1368.
- SALTZMAN, B. & VERNEKAR, A. D. - 1971** - An equilibrium solution for axially-symmetric component of the Earth's macroclimate. Journal of Geophysical Research, **76**: 1498-1524.
- SELLERS, P. J., MINTZ, Y., SUD, Y. C. & DALCHER, A. - 1986** - A simple biosphere (SiB) model for use in general circulation models. Journal of The Atmospheric Sciences, **43**: 505-531.
- PITMAN, A. J. - 1988** - A new parameterization of land surface for use in general circulation models. PhD. Thesis, University of Liverpool, Liverpool, 481 pp.
- VAREJÃO-SILVA, M. A., FRANCHITO, S. H. & RAO, V. B. - 1998** - A coupled biosphere-atmosphere climate model suitable for studies of climate change due to land surface alterations. Journal of Climate, **11**: 1749-1767.

ZHANG, T. - 1994 - Sensitivity properties of a biosphere model based on BATS and a statistical-dynamical model. *Journal of Climate*, 7: 891-913.

APPENDIX A

Method to solve the closed system of equations of the biosphere model.

Substitution of expressions (9), (11), (13), (20) and the flux formulations given in Tabs. 1 and 2 into Eqs. (1), (8), (11) and (22) gives:

$$\psi_{24} T_{sv} + \psi_{22} T_{sv}^4 - \psi_{18} T_f^4 + \psi_3 T_{af} + \psi_4 q_{af} + \psi_5 q_{gs} + \psi_{23} = 0 \quad (A1)$$

$$\psi_3 T_{sv} + \psi_7 T_f + \psi_8 T_{af} + \psi_9 = 0 \quad (A2)$$

$$Y(\psi_{10} T_{af} + \psi_{14}) q_{af} / q_{afs} + \psi_{11} q_{af} + \psi_{12} q_{gs} + \psi_{13} q_{fs} = 0 \quad (A3)$$

$$\psi_{18} T_{sv}^4 + \psi_7 T_f + \psi_{19} T_f^4 - \psi_7 T_{af} + \psi_{20} (q_{fs} - q_{af}) + \psi_{21} = 0 \quad (A4)$$

where the coefficients ψ_i , $i = 1, \dots, 24$ are given in Tab. A1.

The saturated water vapor mixing ratio of the foliage air layer is calculated using:

$$q_{afs} = (0.622/1000) 6.1078 \exp[A(T_{af} - 273.16)/(T_{af} - B)] \quad (A5)$$

and the the saturated mixing ratio of water vapor at the surface (q_{gs}) and the saturated mixing ratio at the foliage temperature (q_{fs}) are obtained using the same Eq. (A5), but substituting T_{af} by T_{sv} and T_f , respectively.

In Eq. (A5) A and B are constants which depend on temperature:

$$\begin{aligned} A &= 21.874 ; B = 7.66 \quad \text{if } T \leq 273.16 \\ A &= 17.269 ; B = 35.86 \quad \text{if } T > 273.16 \end{aligned} \quad (A6)$$

Eqs. (A1)-(A4), with the auxiliary relations for the saturated water vapor mixing ratio (Eq. A5) constitute a closed system of nonlinear equations which must be solved using an iterative method. In the present paper, we used a Newton-Raphson method for the simultaneous solution of nonlinear equation system (Demidovich & Maron, 1976). In this method, if E , x and W represent the solution vector of n equations of the system, the solution vector of n unknown variables, and the jacobian of the system, respectively, i.e.:

$$E = (E_1, E_2, \dots, E_n) \quad (A7)$$

$$x = (x_1, x_2, \dots, x_n) \quad (A8)$$

$$W = \begin{bmatrix} \partial E_1 / \partial x_1 & \partial E_1 / \partial x_2 & \dots & \partial E_1 / \partial x_n \\ \partial E_2 / \partial x_1 & \partial E_2 / \partial x_2 & \dots & \partial E_2 / \partial x_n \\ \dots & \dots & \dots & \dots \\ \partial E_n / \partial x_1 & \partial E_n / \partial x_2 & \dots & \partial E_n / \partial x_n \end{bmatrix} \quad (A9)$$

then, the approximated solution in the interaction $P + 1$ is obtained by:

$$x^{(P+1)} = x^{(P)} - W^{-1} E(x^{(P)}) \dot{x}^{(P)} \quad (A10)$$

for $P = 0, 1, 2, \dots$, where W^{-1} is the inverted matrix of the jacobian W .

It was assumed as the initial interaction ($P = 0$) of the successive approximation process:

$$T_{sv}^{(0)} = T_f^{(0)} = T_{af}^{(0)} = T_{DL}$$

and

$$q_{gs}^{(0)} = q_{afs}^{(0)} = q_{fs}^{(0)} = q_s(T_{DL}) \quad (A11)$$

Received: August, 1997

Accepted: September, 1998

TESTES DE SENSIBILIDADE COM UM MODELO DE BIOSFERA BASEADO NO ESQUEMA BATS, ÚTIL PARA SER ACOPLADO A UM MODELO CLIMÁTICO SIMPLES

A atmosfera é um elemento interativo do sistema climático. Assim, há a necessidade de se desenvolver um modelo de biosfera interativa para simular as mudanças climáticas de longo prazo. É difícil projetar um modelo interativo que simule realisticamente todos os mecanismos de realimentação entre a biosfera e os outros elementos do sistema climático porque há falta ainda do conhecimento dos processos dentro da biosfera. Neste contexto, modelos compreensivos como o BATS (Esquema de Transferência Biosfera-Atmosfera) são muito úteis. Embora estes modelos são mais simples que a atmosfera real, eles são baseados em simplificações razoáveis, que incluem um tratamento adequado dos processos de superfícies. BATS foi originalmente desenvolvido para modelos de circulação geral. Contudo, a inclusão do BATS em um modelo simples, tal como os modelos estatístico-dinâmicos (MED), é muito útil para investigar mudanças climáticas devido à alterações na superfície da terra pois este tipo de modelo grandemente simplifica a análise e ajuda a identificar mecanismos bio-geofísicos.

Neste trabalho, é descrito um modelo de biosfera baseado no BATS, útil para acoplamento com modelos mais simples. Neste modelo as equações do BATS são adaptadas às formulações dos fluxos de energia de um MED global, de duas camadas e de equações primitivas. O modelo de biosfera é rodado desacoplado do MED para realização de testes de sensibilidade a respeito do comportamento das variáveis do modelo em relação à parâmetros descritos do modelo e tipos de vegetação contrastantes, tais como floresta perenifolia e pastagem. Embora haja muitos parâmetros no modelo de biosfera, atenção especial é dada aos efeitos das variações da fração de área coberta pela vegetação (σ_f) e da disponibilidade de água na superfície (f_g). Isto é necessário pois o coeficiente de arrasto e o albedo são fortemente relacionados com σ_f e os fluxos de calor sensível e latente são muito sensíveis a f_g . As variações de σ_f de 0 a 1 é de particular interesse porque representa a transição gra-

dual de solo completamente desnudo para a superfície completamente coberta por vegetação. Desta forma, são considerados ambos os efeitos do reflorestamento como do desflorestamento.

Os resultados mostram que a temperatura da superfície do solo aumenta, em ambos os tipos de vegetação, com o decréscimo da área fracional da cobertura vegetal devido à menor absorção do fluxo de radiação solar. À medida que a interceptação aumenta, a camada de ar na folhagem úmida impede a evaporação de água no solo, de forma que há um aumento da temperatura da superfície do solo. A temperatura da superfície é menor na floresta em relação à pastagem devido ao efeito da rugosidade da superfície. No caso de solo seco, a energia disponível aumenta com o aumento da área fracional da cobertura vegetal pois o fluxo de calor latente aumenta rapidamente, enquanto que o fluxo de calor sensível diminui lentamente. No caso de solo completamente úmido (saturado) a dependência da energia disponível em relação à interceptação é reduzida devido ao efeito da evaporação de água na superfície, que aumenta o fluxo de calor latente mesmo que a interceptação seja pequena ou nula.

Testes de sensibilidade são feitos a respeito do fator Y , introduzido na expressão do fluxo de vapor d'água para a atmosfera a fim de ajustar a partição da energia disponível em calor sensível e latente. Os resultados mostram que o fluxo de calor latente (sensível) aumenta (diminui) com o aumento de Y . Embora a variação de Y modifica a razão de Bowen, não há mudança da partição da evapotranspiração em seus termos componentes.

Um fator ζ é inserido na expressão que indica a área fracional das folhas cobertas por água para considerar o efeito da parte da vegetação predominantemente porosa. Os menores valores de ζ mostram melhores resultados com respeito aos termos componentes da evapotranspiração. Contudo, os fluxos total de vapor d'água para a atmosfera não se altera com ζ .

NOTES ABOUT THE AUTHORS *NOTAS SOBRE OS AUTORES*

SENSITIVITY TESTS WITH A BIOSPHERE MODEL BASED ON BATS, SUITABLE FOR COUPLING WITH A SIMPLE CLIMATIC MODEL

Sergio Henrique Franchito

Bsc (Physics) from the Universidade Estadual Paulista Julio de Mesquita (UNESP), Rio Claro, SP, 1976.

Msc, Meteorology, from the Instituto Nacional de Pesquisas Espaciais (INPE), São José dos Campos, SP, 1980.

Ph.D. (Meteorology) from the Instituto Nacional de Pesquisas Espaciais (INPE), São José dos Campos, SP, 1989.

Research Activities: Researcher at INPE since 1980.

Areas of Interest: Climatic Modeling, Climate Dynamics, Mesoscale Modeling.

Vadlamudi Brahmananda Rao

Bsc (Physics) from the Andhra University, India, 1960.

Msc (Tech), Meteorology and Oceanography from the Andhra University, India, 1963.

Ph.D., Meteorology, Andhra University, India, 1969.

Research Activities: Researcher at Indian Institute of

Tropical Meteorology, 1965-1969. Researcher at INPE since 1971.

Areas of Interest: Tropical Meteorology, Climate Dynamics, Upper Atmosphere.

Mário Adelmo Varejão-Silva

Bsc (Agronomy) from the Escola de Agronomia do Nordeste, Areias, Paraíba, 1965.

Msc, Meteorology from the Instituto Nacional de Pesquisas Espaciais (INPE), São José dos Campos, SP, 1976.

Ph. D., Meteorology at Instituto Nacional de Pesquisas Espaciais (INPE), São José dos Campos, SP, 1996.

Research Activities: Agrometeorologist at Superintendência do Desenvolvimento do Nordeste, Recife, PE, 1966-1977. Professor of Meteorology at Universidade Federal da Paraíba, Campina Grande, 1977-1985. Professor of Meteorology at Universidade Federal Rural de Pernambuco, Recife, PE, 1985-1997.

Areas of Interest: Agrometeorology, Climatology.

SIMULATION OF SPECTRAL PLANETARY REFLECTANCE OF TARGETS

Morgana Lígia de Farias Freire

Bsc (Physics) at Universidade Estadual da Paraíba (UEPb), Campina Grande, Pb, 1993

Msc (Meteorology) at Universidade Federal da Paraíba (UFPb), Campina Grande, Pb, 1996

Research Activities: Professor of Physics at Universidade Estadual da Paraíba since 1997.

Areas de Interest: Physics, Atmospheric Radiation, Remote Sensing

Eduardo Jorge de Brito Bastos

Bsc (Meteorology) at Universidade Federal da Paraíba (UFPb), Campina Grande, Pb, 1979.

Msc (Meteorology) at Universidade Federal da Paraíba (UFPb), Campina Grande, Pb, 1986.

Ph.D. (Meteorology) at Instituto Nacional de Pesquisas Espaciais (INPE), São José dos Campos, SP, 1994.

Research Activities: Professor at UFPb since 1979 and Visitant Research at INPE since 1994

Areas of Interest: Atmospheric Radiation, Satellite Meteorology, Remote Sensing